

PARAMETER SENSITIVITY ANALYSIS AND OPTIMIZATION OF VIBRATION ENERGY OF A HYBRID ENERGY-REGENERATIVE SUSPENSION

JIAJIA WANG, LONG CHEN, RUOCHEN WANG, XIANGPENG MENG, DEHUA SHI

School of Automotive and Traffic Engineering, Jiangsu University, Zhenjiang, China

e-mail: chenlong@ujs.edu.cn

To reveal energy transfer characteristics of a hybrid energy-regenerative suspension during the driving process, a two-degree-of-freedom suspension model considering the nonlinearity of the tire damping is proposed. Meanwhile, energy efficiency, the unified index for all driving conditions, is obtained, and its sensitivity to different influencing factors is deeply analyzed. The results obviously show that the influence of the same structural parameters on energy efficiency varies with the excitation frequency of the road surface, especially at 1 Hz and 10 Hz. Based on these results, the damping values under different frequency bands are optimized to balance the energy recovery and dynamic performances of the suspension.

Keywords: hybrid energy-regenerative suspension, vibration energy, energy efficiency, sensitivity, optimal damping

1. Introduction

With the increasing shortage of energy all over the world, the problem of vehicle energy-saving is a common challenge faced by the international automotive community. According to the US DOE data, approximately 70% of oil is consumed in transportation every year. Therefore, how to effectively improve vehicle fuel economy (Balzarini *et al.*, 2017; Bento *et al.*, 2017) is a key issue to be urgently solved.

The emergence of energy regeneration technology in the 1890s provided new ideas for solving this problem. The development and application of technologies such as braking energy regeneration (Ko *et al.*, 2015; Lv *et al.*, 2015; Li *et al.*, 2016) and thermoelectric waste heat recovery (Hsu *et al.*, 2011; Yu *et al.*, 2015; Huang and Xu, 2017) have greatly eased energy pressure. To achieve more comprehensive energy-saving efficiency for automobiles, domestic and foreign scholars have carried out renewable energy feasibility studies in another area-automobile vibration energy recovery since the 1970s (Shi *et al.*, 2016; David and Bobrovsky, 2011; Nakano *et al.*, 2003; Singal and Rajamani, 2013). Thanks to its simple structure, fast response, large controllable bandwidth, no intermediate transmission mechanism and mechanical wear, the linear motor (Mo *et al.*, 2017; Dong *et al.*, 2017; Abdalla *et al.*, 2017) has broad prospects as a power recovery mechanism for the suspension.

Browne fully evaluated that four hydraulic dampers in the suspension dissipate approximately 40 to 60 W of power when the car is driving in urban road conditions (Browne and Hamburg, 1986). Li demonstrated through prototype tests that a vehicle loaded with four specially structured energy-recovery devices can recover up to 67.5 W of energy when driving on a relatively smooth road at 30 km/h (Li *et al.*, 2013). Zuo pointed out that when the suspension vibration speed reaches 0.25 m/s-0.5 m/s, the recoverable energy is as high as 16-64 W (Zuo *et al.*, 2010). All of the above studies show that the vibration energy dissipated by a hydraulic damper is

considerable, and the recovery potential is great when the vehicle suspension is resisting road impacts.

However, the amount of energy recovery is restricted by many factors. All the above studies have neglected the equivalent damping of automobile tires in the actual driving process. As the excitation frequency of pavement increases, the damping energy consumption has a significant impact on the energy recovery of a linear motor and should not be ignored. Additionally, only a few scholars have conducted a rough study of suspension energy regeneration, and most of them use power recovery instead of energy efficiency to measure the energy supply characteristics of the suspension, but this measure is only valid under the same driving conditions.

In summary, suspension vibration energy recovery is indeed feasible, and is of great significance for improving vehicle fuel efficiency. However, it is worth noting that the influence of suspension energy recovery on the vehicle dynamics performance is not negligible (Ataei *et al.*, 2017). Therefore, how to effectively coordinate the relationship between the energy regeneration and vehicle dynamic performance is a key issue in the suspension design. To realize the comprehensive optimization of energy recovery and the dynamic characteristics of the hybrid energy-regenerative suspension, this paper first explores its energy regeneration potential and related influencing factors, and then optimizes the key parameters based on its influence. Finally, dual verification ensures through simulation and experiment that the optimized suspension combines comfort, safety and vibration energy recovery.

Based on the above, this paper proposes a hybrid energy-regenerative suspension structure with a spring-hydraulic damper and a linear motor connected in parallel. The damping of the tire has been taken into consideration and its vibration energy transfer characteristics have been studied. The energy recovery index, energy efficiency, is proposed and its sensitivity to different influencing factors has been analyzed in depth. According to this sensitivity, the key vehicle parameters that can effectively balance the energy efficiency and dynamic performance are later designed.

The structure of this paper is as follows: Section 2 builds a two-degree-of-freedom suspension model. Section 3 investigates the transmission energy characteristics of the suspension and its energy efficiency sensitivity; Section 4 optimizes the key influencing parameters based on this sensitivity, considering energy-recovery and dynamic performance. Section 5 conducts a series of experimental studies and finally Section 6 concludes the research of this paper.

2. Hybrid suspension model

Most domestic and foreign scholars ignore tire damping when they study electromagnetic suspension energy recovery, which in fact is not always small and varies greatly with the frequency of road excitation (Chen and Jin, 2004; Xue *et al.*, 1994). From these references it can be seen that the tire damping coefficient decreases sharply with an excitation frequency increase, and the two satisfy the following relationship

$$c_t = \alpha f^\beta \quad (2.1)$$

Among them, α and β are regression coefficients. In this paper, $\alpha = 2283$ and $\beta = -0.9667$.

As shown in Fig. 1, even if the excitation frequency is as high as 10 Hz, the damping coefficient is maintained at approximately 382 N·s/m. Therefore, in order to truly and accurately reflect the overall vibration energy dissipation of the suspension, the impact of the tire on its energy distribution cannot be ignored.

A vehicle is a complex vibration system that should be simplified based on the problem being analyzed. Assuming that the vehicle body mass is a rigid three-dimensional model, when discussing vehicle ride comfort, the body mass of this three-dimensional model mainly considers

three degrees of freedom: vertical, roll and pitch, and four wheels have four degrees of freedom, adding up to seven degrees of freedom. When the vehicle is symmetrical to its axis and the unevenness function of the left and right ruts is the same, the vehicle has only vertical and pitching vibration, which is simplified to a plane model with 4 degrees of freedom. When the suspension mass distribution coefficient is close to 1, the vertical vibration of the front and rear suspension systems is almost independent, so it can be simplified to the two-degree-of-freedom vibration system shown in Fig. 2. Although the vehicle quarter model is simple, it contains most of the basic features of the practical problems and has few system description parameters, so the calculation is simple and reflects the main characteristics of the real suspension.

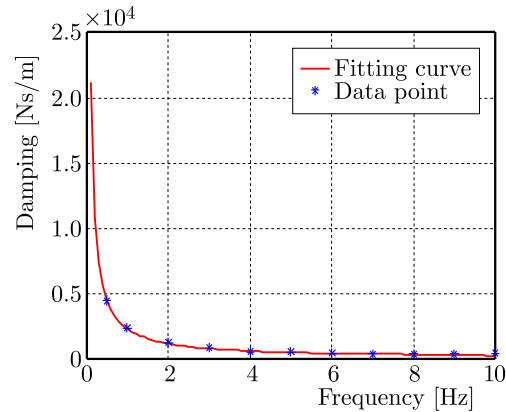


Fig. 1. Relationship between tire damping and frequency

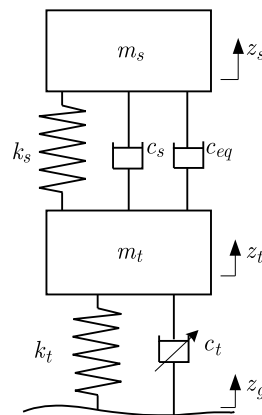


Fig. 2. Hybrid suspension model. The arrow indicates nonlinearity of the damper

Thus, a two-degree-of-freedom vertical hybrid suspension model considers the tire damping nonlinearity shown in Fig. 2. In the figure, the suspension mass m_s is composed of the body, frame and its assembly. The suspension mass is connected to the axle and the wheel by the suspension spring k_s , the damper c_s and the linear motor (equivalent damping is c_{eq}). The unsprung mass of the wheel and axle is m_t , and the wheel is supported on an uneven road by a tire having a certain elasticity k_t and damping c_t . It is worth noting that c_s as well as the equivalent damping of the motor c_{eq} are considered as linear, while c_t is a nonlinear damping. The vertical displacement coordinates of the body and the wheel are z_s and z_t , respectively, and the coordinate origins are selected at their respective equilibrium positions. z_g is the input road roughness function.

The motor selected for the hybrid suspension needs to meet normal operation requirements of the entire suspension system. The volume of the motor should be as small as needed to operate

in a limited space between the vehicle body and the wheel. A permanent magnet synchronous linear motor is more suitable for its small volume, high power factor, fast response and high cost performance.

According to the model, its kinetic equation can be expressed as

$$\begin{bmatrix} m_s & 0 \\ 0 & m_t \end{bmatrix} \begin{Bmatrix} \ddot{z}_s \\ \ddot{z}_t \end{Bmatrix} + \begin{bmatrix} c_s & -c_s \\ -c_s & c_s + c_t \end{bmatrix} \begin{Bmatrix} \dot{z}_s \\ \dot{z}_t \end{Bmatrix} + \begin{bmatrix} k_s & -k_s \\ -k_s & k_s + k_t \end{bmatrix} \begin{Bmatrix} z_s \\ z_t \end{Bmatrix} = \begin{Bmatrix} -F \\ c_t \dot{z}_g + k_t z_g + F \end{Bmatrix} \quad (2.2)$$

3. Sensitivity analysis of energy efficiency at different frequencies

3.1. Energy transfer characteristics

When a linear motor works in the generator mode to recover energy, the permanent magnet and the coil will generate relative motion. According to Faraday's law of electromagnetic induction, the coil will generate an induced electromotive force and thereby convert the vibration energy into electric energy. At the same time, the motor will generate an electromagnetic damping force that always hinders the relative movement of the permanent magnet and coil. Thus, the linear motor is equivalent to a passive damper, and its equivalent damping (see the appendix for details) and the damping force can be expressed as

$$c_{eq} = \frac{k_e k_f}{R_m} \quad F = c_{eq}(\dot{z}_s - \dot{z}_t) \quad (3.1)$$

System parameters are shown in Table 1.

Table 1. Parameters of the system

Parameter	Symbol [unit]	Value
Sprung mass	m_s [kg]	250
Unsprung mass	m_t [kg]	45
Spring stiffness	k_s [N/m]	16000
Tire stiffness	k_t [N/m]	160000
Linear motor back-EMF coefficient	k_e [V·s/m]	62.6
Linear motor thrust coefficient	k_f [N/A]	77.9
Motor internal resistance	R [Ω]	10.16

Generally, the random excitation of the road surface can be considered as a superposition of sine or cosine functions with random phases. This paper focuses on the balance between energy recovery characteristics and the suspension dynamic performance (considering the tire damping nonlinearity) under the excitation input of the road. Therefore, only a single sine wave excitation can be used to decouple the tire damping from the road surface excitation, and the tire damping can be determined by Fig. 2 on the basis of quickly identifying the excitation frequency for subsequent performance studies. However, if the random excitation is used and the excitation frequency cannot be identified in real time, the purpose of considering the tire damping nonlinearity cannot be achieved.

Therefore, when the road surface is a harmonic input, it can be deduced using Cramer's law

$$\begin{bmatrix} k_s + j\omega(c_s + c_{eq}) - \omega^2 m_s & -k_s - j\omega(c_s + c_{eq}) \\ -k_s - j\omega(c_s + c_{eq}) & (k_s + k_t) + j\omega(c_s + c_{eq} + c_t) - \omega^2 m_t \end{bmatrix} \begin{Bmatrix} z_1 \\ z_2 \end{Bmatrix} = \begin{Bmatrix} 0 \\ j\omega c_t z_3 + k_t z_3 \end{Bmatrix} \quad (3.2)$$

and

$$z_1 = \frac{\Delta_1}{\Delta_0} = \frac{\begin{vmatrix} 0 & -k_s - j\omega(c_s + c_{eq}) \\ j\omega c_t z_3 + k_t z_3 & (k_s + k_t) + j\omega(c_s + c_{eq} + c_t) - \omega^2 m_t \end{vmatrix}}{\begin{vmatrix} k_s + j\omega(c_s + c_{eq}) - \omega^2 m_s & -k_s - j\omega(c_s + c_{eq}) \\ -k_s - j\omega(c_s + c_{eq}) & (k_s + k_t) + j\omega(c_s + c_{eq} + c_t) - \omega^2 m_t \end{vmatrix}} \tag{3.3}$$

$$z_2 = \frac{\Delta_2}{\Delta_0} = \frac{\begin{vmatrix} k_s + j\omega(c_s + c_{eq}) - \omega^2 m_s & 0 \\ -k_s - j\omega(c_s + c_{eq}) & j\omega c_t z_3 + k_t z_3 \end{vmatrix}}{\begin{vmatrix} k_s + j\omega(c_s + c_{eq}) - \omega^2 m_s & -k_s - j\omega(c_s + c_{eq}) \\ -k_s - j\omega(c_s + c_{eq}) & (k_s + k_t) + j\omega(c_s + c_{eq} + c_t) - \omega^2 m_t \end{vmatrix}}$$

While

$$\begin{aligned} \Delta_0 &= [k_s k_t - \omega^2 m_t k_s - \omega^2 m_s k_s - \omega^2 m_s k_t + \omega^4 m_s m_t - \omega^2 (c_s + c_{eq}) c_t] \\ &\quad + \{\omega [k_s c_t + k_t (c_s + c_{eq}) - \omega^2 m_s (c_s + c_{eq}) - \omega^2 m_s c_t - \omega^2 m_t (c_s + c_{eq})] j\} \\ \Delta_1 &= [k_s k_t z_3 - \omega^2 (c_s + c_{eq}) c_t z_3] + \{\omega [k_s c_t z_3 + k_t (c_s + c_{eq}) z_3] j\} \\ \Delta_2 &= [k_s k_t z_3 - \omega^2 (c_s + c_{eq}) c_t z_3 - \omega^2 m_s k_t z_3] + \{\omega [k_s c_t z_3 + k_t z_3 (c_s + c_{eq}) - \omega^2 m_s c_t z_3] j\} \end{aligned} \tag{3.4}$$

Assuming the relative displacement between the sprung and the unsprung mass is x_1 , and the dynamic deformation of the tire is x_2 , when $z_g = z_3 \sin(\omega t)$, the energy dissipated by the hydraulic damper c_s , tire c_t and the recoverable energy of the linear motor are

$$\begin{aligned} p_{c_s} &= \frac{c_s \omega^2 |x_1|^2}{2} = \frac{c_s \omega^2}{2} \left| \frac{\Delta_1}{\Delta_0} - \frac{\Delta_2}{\Delta_0} \right|^2 & p_{c_t} &= \frac{c_t \omega^2 |x_2|^2}{2} = \frac{c_t \omega^2}{2} \left| \frac{\Delta_2}{\Delta_0} - z_3 \right|^2 \\ p_{out} &= \frac{c_{eq} \omega^2 |x_1|^2}{2} = \frac{c_{eq} \omega^2}{2} \left| \frac{\Delta_1}{\Delta_0} - \frac{\Delta_2}{\Delta_0} \right|^2 \end{aligned} \tag{3.5}$$

Based on the above formula (3.5), the energy efficiency η , an index for measuring the energy recovery of a hybrid suspension, is proposed as follows

$$\eta = \frac{p_{out}}{p_{c_t} + p_{c_s} + p_{out}} \tag{3.6}$$

3.2. Sensitivity analysis

When the vehicle is driving on an uneven road, the energy recovery characteristics of the suspension could be affected by the external environment (especially excitation frequency) and the internal structural parameters of the vehicle (sprung mass, unsprung mass, spring stiffness, tire equivalent stiffness, shock absorber damping). Figure 3 depicts the effects of each single suspension structural parameter on vibration energy recovery in different frequency domains. As shown in Fig. 3a, the sprung mass has almost no effect on the suspension vibration energy recovery. The effect of the unsprung mass on low frequency input is insignificant, whereas at higher frequency the power feeding efficiency of the motor gradually decreases as it increases. In addition, the damping coefficient and energy efficiency are negatively correlated. It is worth noting that the downward trend in the low frequency region is more intense.

The spring stiffness tends to increase the energy efficiency slightly in the middle and high frequency regions, and it decreases significantly in the low frequency region. In contrast, the energy efficiency shows a significant growth trend in the high frequency area due to tire stiffness, but the trend is not obvious in the low frequency area. This is caused by the tire resonance phenomenon. As the tire stiffness increases, its dynamic deformation decreases, and the vibration energy of the tire equivalent damping dissipates. Therefore, with the same road input, according

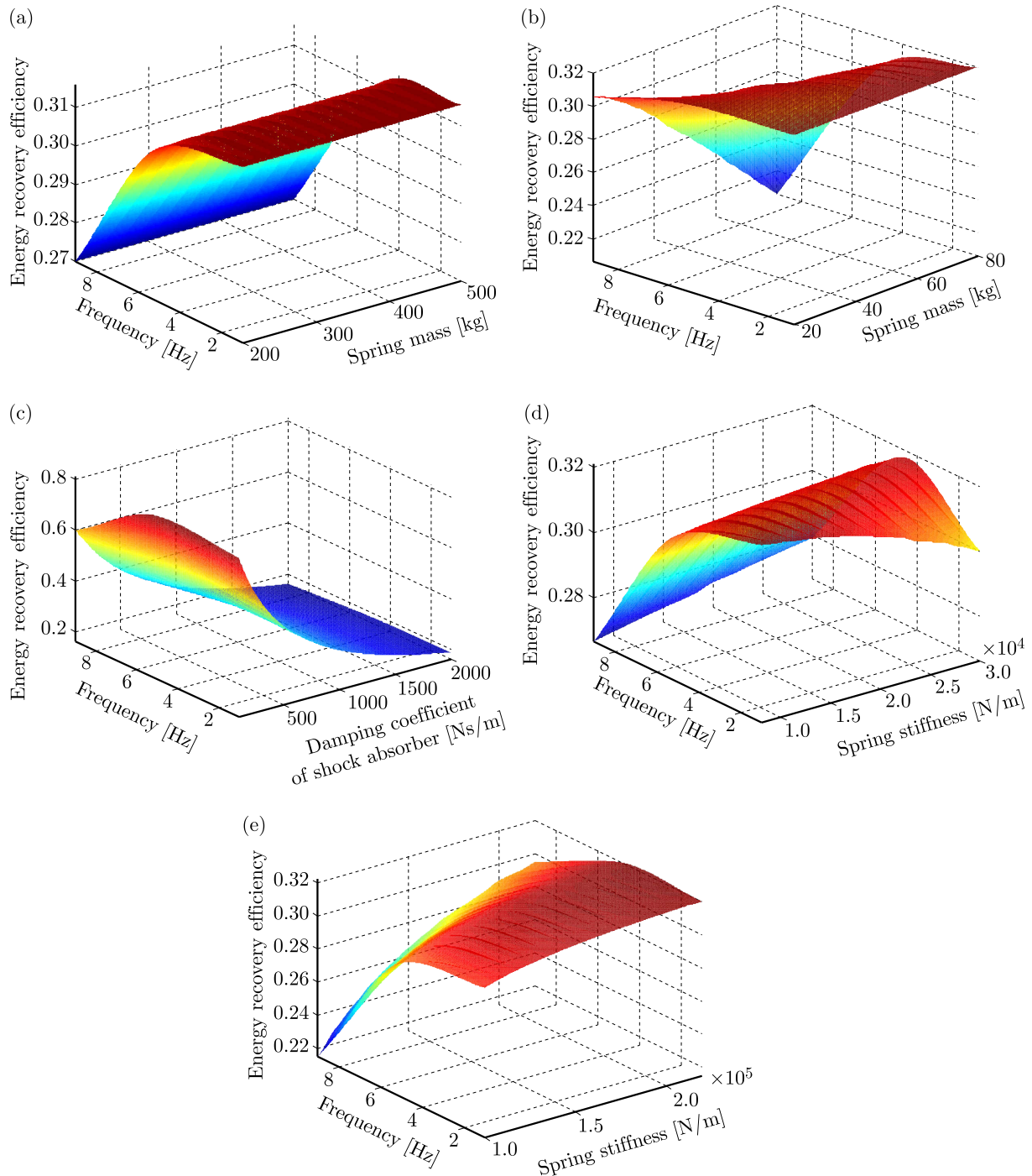


Fig. 3. Influence of tire stiffness on energy efficiency: (a) sprung mass, (b) unsprung mass, (c) damping coefficient, (d) spring stiffness, (e) tire stiffness

to energy conservation, when energy dissipation of the hydraulic damper takes place, the linear motor recyclable energy increases with a simultaneous rise in the energy efficiency. In general, the damping coefficients of different tires under different inflation pressures are different, but the nonlinear tendency is basically the same, that is, the damping coefficient c_t decreases sharply with an increase in the excitation frequency. Therefore, there will be some differences in the sensitivity analysis of the suspension regeneration performance for different tires, but the laws presented are basically the same.

It is comprehensively concluded that the structural parameters such as the unsprung mass, spring stiffness and tire stiffness have significantly different effects on the linear motor energy

efficiency when the excitation frequencies of the road surface input are different in the above figures, especially for the influence of spring stiffness. These results indicate that we need to consider the optimal parameters of the equilibrium suspension energy efficiency and dynamic performance in important frequency bands during the parameter design process.

4. Key parameter optimization

From the sensitivity analysis, it can be seen that the energy efficiency has the highest sensitivity to the shock absorber damping coefficient in the low and high frequency areas, and the energy efficiency decreases sharply with the damping value increase. From the perspective of vehicle dynamics, the damper can accelerate vibration attenuation of the frame and body and improve ride comfort. In addition, the resonance frequency could greatly reduce ride comfort and tire grounding, so how to effectively balance the adverse effects of the vehicle body and wheel resonance as well as the energy efficiency is the key problem to be solved in this paper.

This paper will mainly explore the optimal damping coefficient of shock absorbers considering the dynamic performance and energy recovery when the external excitation frequencies are set to the body resonance frequency of 1 Hz and the wheel resonance frequency of 10 Hz respectively. In terms of the suspension system, the object of optimization has good energy recovery efficiency, ride comfort and driving safety, that is, high energy recovery efficiency as well as small vehicle body acceleration and dynamic tire load. Thus, the goal-function can be expressed as

$$J = \lim_{T \rightarrow \infty} \frac{1}{T} \int_0^T [r_1 \eta^2 + r_2 \ddot{z}_s^2 + r_3 k_t^2 (z_t - z_g)^2] dt \quad (4.1)$$

The constraints are related with the non-optimized damping value of 1000, when the same external excitation is applied, the vehicle body acceleration peak value of 4 and the tire dynamic load peak value of 3000. These are the reference limits

$$0 \leq \eta \leq 1 \quad 0 \leq \ddot{z}_s \leq 4 \quad 0 \leq k_t(z_t - z_g) \leq 3000 \quad (4.2)$$

where r_1 , r_2 , and r_3 are the performance weighting factors. By choosing different values, one or two performances can be emphasized.

The weight coefficient values selected in this paper are shown in Table 2.

Table 2. The weight coefficient values

Excitation frequency [Hz]	r_1	r_2	r_3
1	$6.3 \cdot 10^4$	$3.4 \cdot 10^4$	0
10	$7.8 \cdot 10^4$	0	$4.8 \cdot 10^4$

The control variable of the system is the damper damping c_s . In the MATLAB programming environment, a function transformed by the objective function and the constraint is used as the mathematical model of the particle swarm optimization algorithm. The population size is set to 100, the learning factor is 2, and the inertia factor is 0.8. Finally, the optimal damper damping values are 400 N·s/m and 500 N·s/m according to the particle swarm optimization algorithm.

As shown in Fig. 4a, when the vehicle is subjected to a sine external excitation with an amplitude of 0.015 m and a frequency of 1 Hz, both the RMS acceleration of the vehicle body and the energy efficiency decrease, and reach the compromise requirement with energy efficiency reaching 53% when the shock absorber damping value is 400 N·s/m.

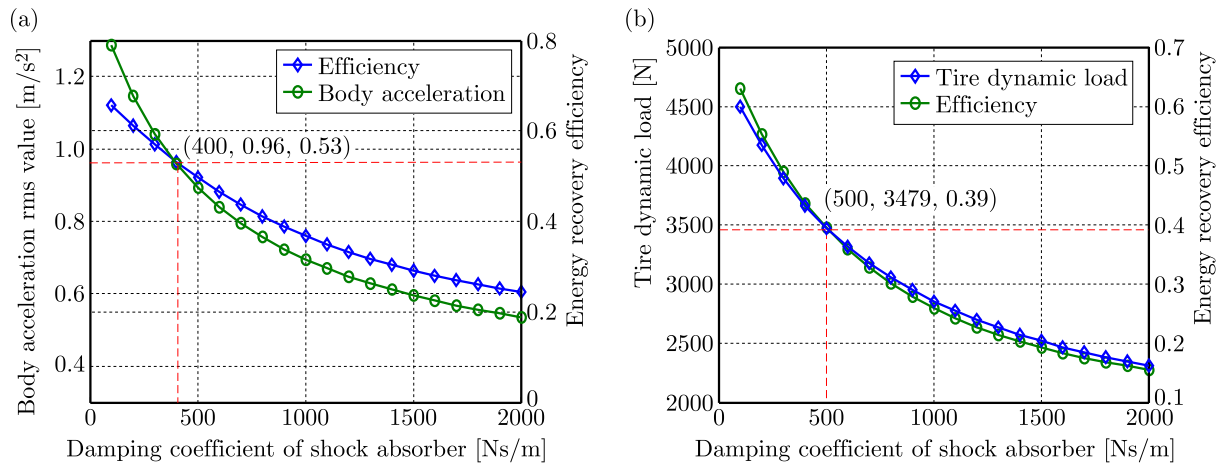


Fig. 4. Relationship between the damping value, energy efficiency, driving safety and ride comfort: (a) 1 Hz, (b) 10 Hz

Figure 4b also describes the variation between the damping value of the shock absorber and the RMS value of the tire dynamic load as well as the energy efficiency when the external excitation is of the same amplitude and with a frequency of 10 Hz. Similarly, it can be seen that both sides achieve a trade-off when the damping value is 500 N·s/m and the energy efficiency is 39%. Therefore, considering the overall comfort of the vehicle, especially the energy efficiency, this paper selects a damping value of 400 N·s/m as the best shock absorber damping coefficient at the expense of minor driving safety (the tire dynamic load deteriorates by 0.06%, but within an acceptable range).

Figure 5 gives simulation results including four segments with amplitudes of 0.015 m, 0.015 m, 0.005 m and 0.005 m, respectively.

5. Experimental research

To verify the correctness and effectiveness of the abovementioned damping optimization, a bench test was performed on an INSTRON 8800 hydraulic servo vibration excitation test stand. This experiment used the equivalent structure of a 1/4 suspension where a linear motor was connected in parallel with a shock absorber. By simulating a sinusoidal road surface input, multiple sets of comparison tests (the optimal damping coefficient 400 N·s/m, the general damping coefficient 1000 N·s/m, and the small damping coefficient 200 N·s/m) were carried out. Usually, a human body on a seat has a sensitive vertical vibration range of 4-12.5 Hz, and the resonance phenomenon will also occur in some automobile body systems below 3 Hz. Based on this, this paper focuses on the selection of 0.5-15 Hz as the important frequency range for suspension performance research. In addition, by analyzing the road interference model for common working conditions (highway, urban highway), it is found that the root mean square value of vertical displacement input is in the range of [0 mm, 20 mm]. To simulate the vehicle authenticity and safety, the corresponding excitation amplitude should be smaller. That is, the amplitude in the range of 0.5 to 7 Hz is 15 mm, and in the range of 8 to 15 Hz it is 5 mm.

Figure 6 shows the overall test design. In this experiment, sinusoidal excitation was used as the road surface input. The excitation frequency and amplitude are shown in Table 3. Considering the positive correlation between the suspension power recovery and the super capacitor voltage, in order to reduce the amount of calculation, the test part uses the capacitor terminal voltage as its measurement index.

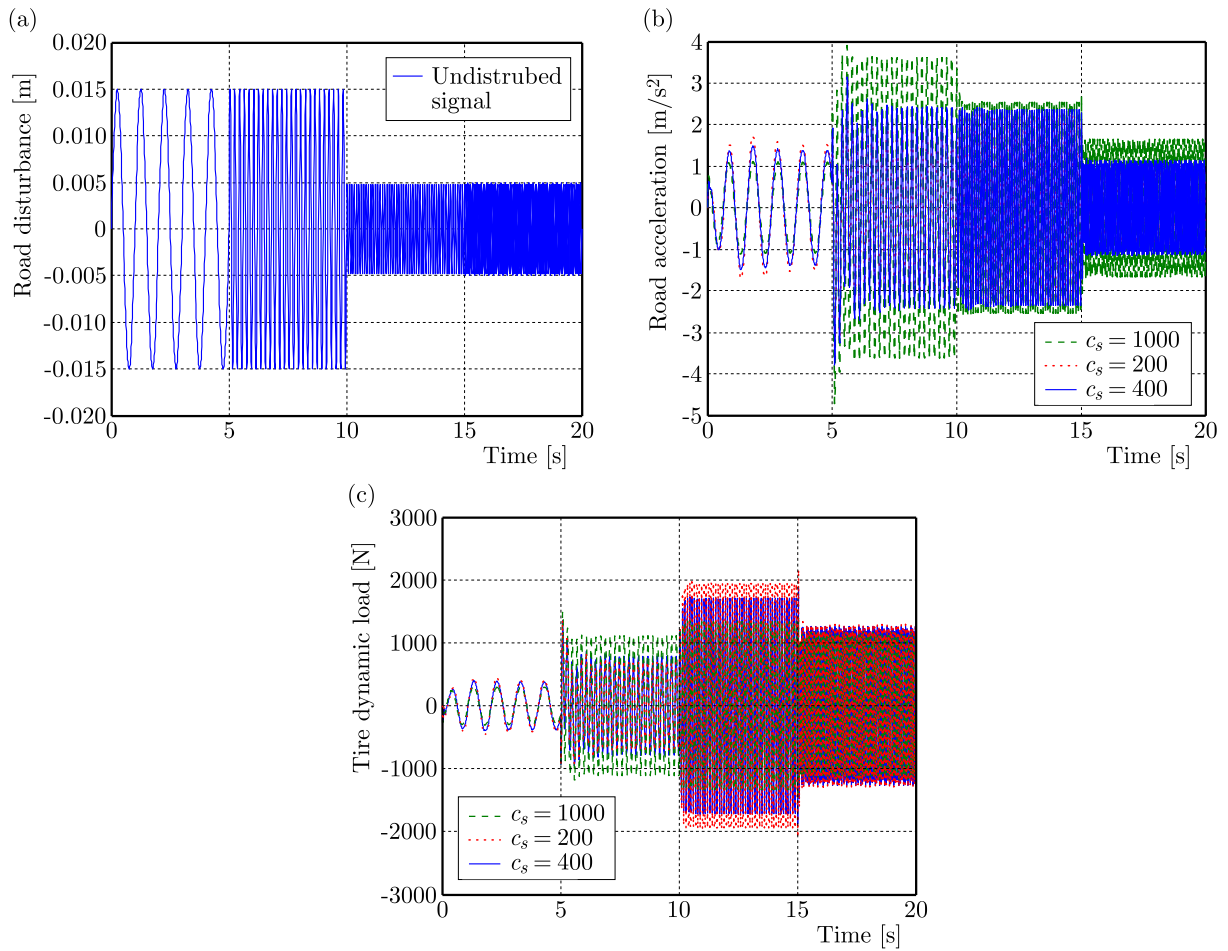


Fig. 5. Sinusoidal simulation: (a) road surface excitation signal, (b) body acceleration response, (c) tire dynamic load response

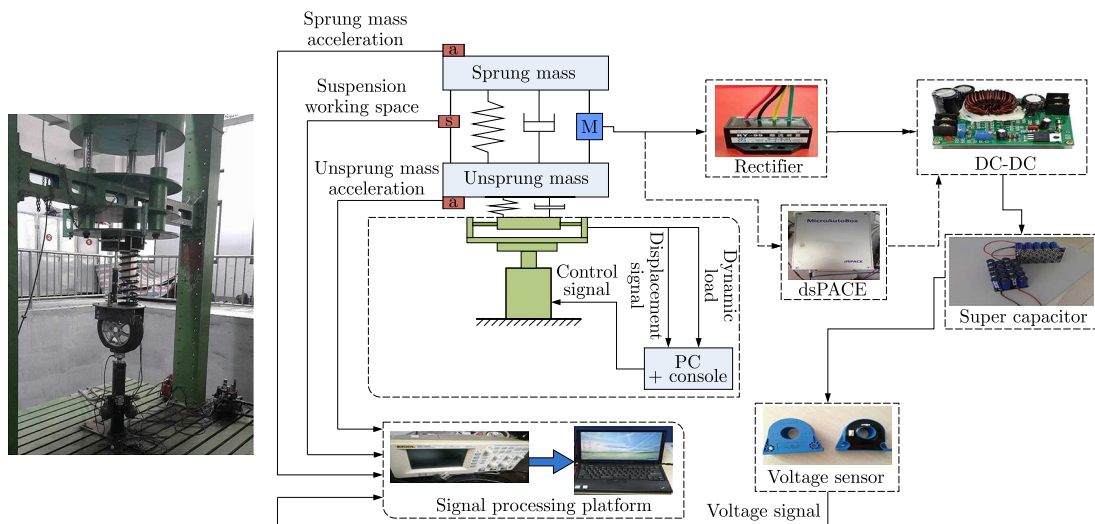


Fig. 6. Schematic diagram of the bench test

Figure 7 shows the corresponding test results with different shock absorbers, where RMS (BA) represents the root mean square of the body acceleration, RMS (TDL) represents the root mean square of the tire dynamic load, and RMS (CV) represents the root mean square of the terminal voltage.

Table 3. Sinusoidal bench test excitation

Excitation frequency [Hz]	Excitation amplitude [mm]
0.5, 1, 2, 3, 4, 5, 6, 7	15
8, 9, 10, 11, 12, 13, 14, 15	5

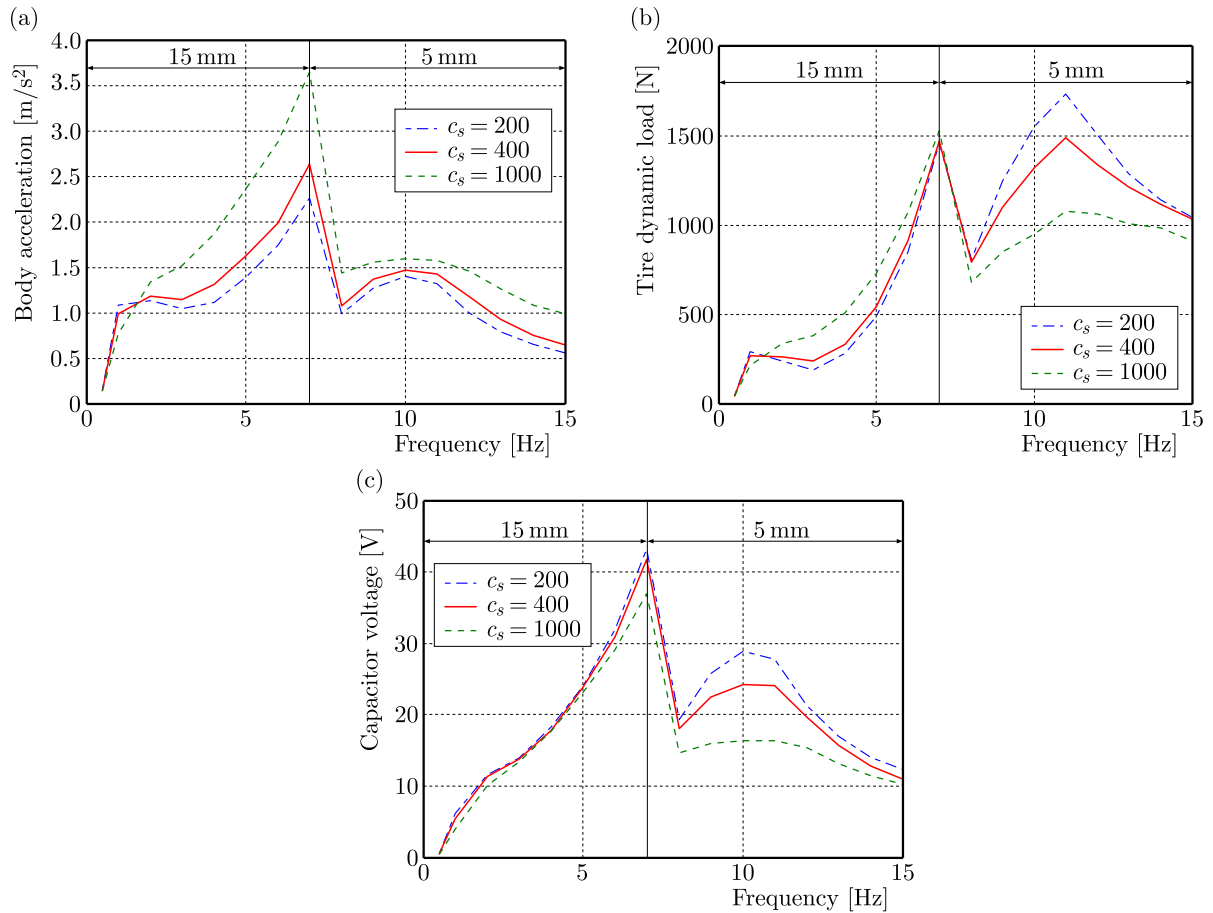


Fig. 7. Comparison of test results among different dampers: (a) RMS (BA), (b) RMS (TDL), (c) RMS (CV)

From the figure, we can conclude that a greater damping value of the shock absorber contributes to improving the overall vehicle ride comfort in the low frequency region, but not for the low-frequency resonance regions. In contrast, the dynamic load of the tire decreases with increasing the damping value in the low frequency and high-frequency resonance regions. Meanwhile, the super capacitor charging voltage is negatively correlated with shock absorber damping. Stated thus, the damping $c_s = 400$ N·s/m can balance energy and dynamic performance throughout the frequency domain.

Otherwise, Fig. 8 gives a comparison between the test and simulation. It is obvious that there are certain errors between the simulation and test. The reason is mainly that the simulation ignores shock absorber nonlinear factors and the linear motor friction resistance, making the actual damping force larger. In contrast, in the simulation, neglecting the loop resistance is considered the primary cause.

Despite the existence of various errors, the test results are in good agreement with the simulation, which verifies the design correctness of the hybrid energy-regenerative suspension system key parameters.

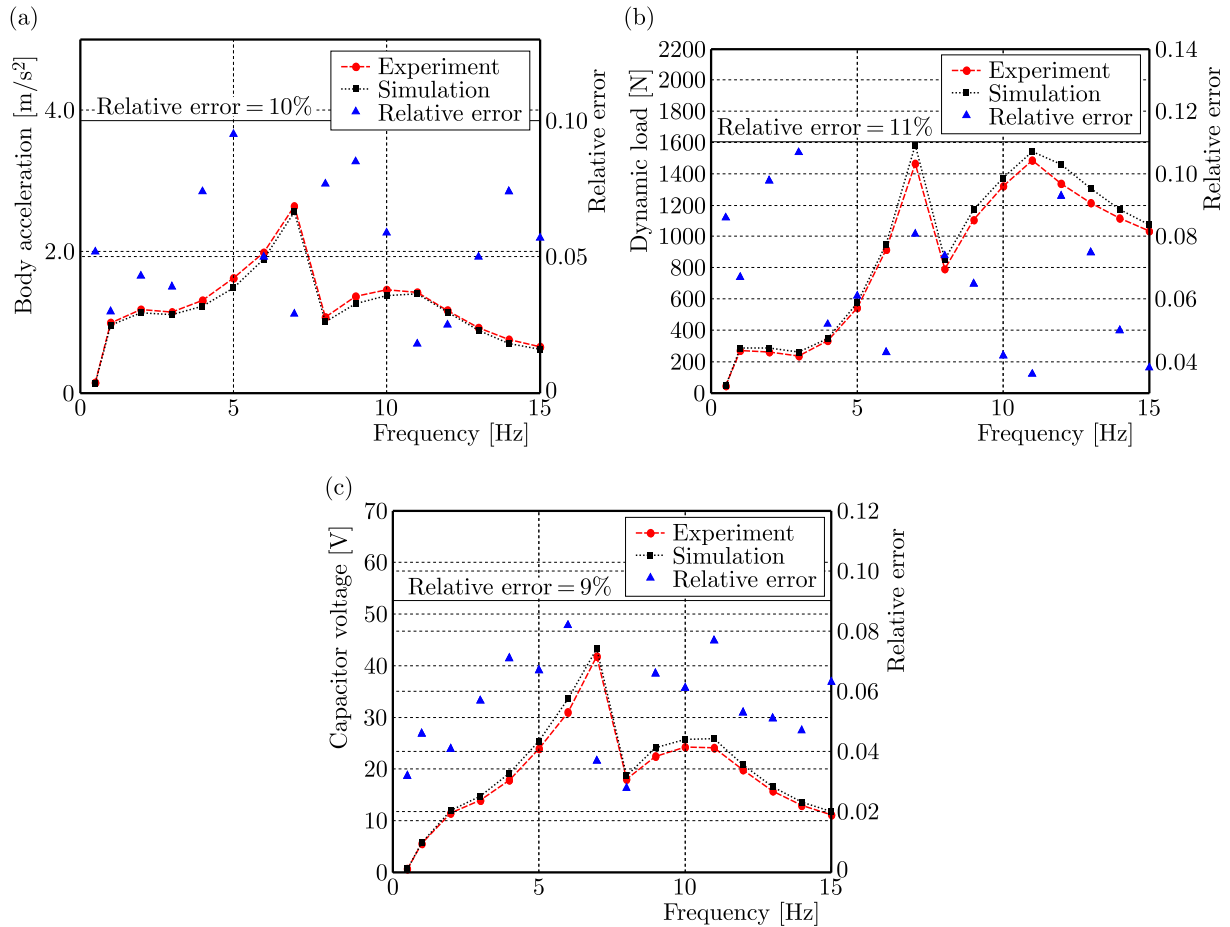


Fig. 8. Comparison of the simulation results with the test: (a) vehicle body acceleration, (b) dynamic load, (c) capacitor terminal voltage

6. Conclusion

- To reveal the energy transfer characteristics of the vehicle suspension system during the vibration process, nonlinear tire damping is introduced, and a two-degree-of-freedom hybrid suspension model is established.
- The expressions of the energy consumption/recovery are deduced for each component of the suspension system under a harmonic excitation, more realistic vehicle vibration energy transfer characteristics are revealed, and the index for measuring the suspension feed energy is given as the energy efficiency. Considering that the suspension power recovery is affected by a variety of internal and external factors at the same time, a sensitive power efficiency parameter analysis is performed. The result shows that the shock absorber damping is the structural parameter with the highest sensitivity.
- Based on the sensitivity of the above parameters, this paper optimizes the damper damping to balance the overall system energy supply and dynamic response. Finally, the correctness of damping optimization has been verified through simulation analysis and test comparison.

Appendix

When the linear motor operates in the generator mode, the induced electromotive force is as follows

$$V_{emf} = -k_e(\dot{z}_s - \dot{z}_t)$$

where k_e is the linear motor back electromotive force coefficient, and z_s and z_t are the vertical displacements of the sprung and the unsprung mass, respectively. At this time, the coil winding current I is

$$I = \frac{k_e(\dot{z}_s - \dot{z}_t)}{R_m}$$

The relationship between the linear motor output force F and the coil winding current I is

$$F = k_f I$$

where R_m is the linear motor internal resistance, and k_f is the thrust coefficient of the linear motor. The simultaneous formula can be obtained as follows

$$F = \frac{k_e k_f (\dot{z}_s - \dot{z}_t)}{R_m} = c_{eq} (\dot{z}_s - \dot{z}_t)$$

That is

$$c_{eq} = \frac{k_e k_f}{R_m}$$

Funding

This work was supported by the National Natural Science Foundation of China (Grant No. 51575240).

References

1. ABDALLA I.I., IBRAHIM T., PERUMAL N., NOR M.N., 2017, Minimization of eddy-current loss in a permanent-magnet tubular linear motor, *International Journal on Advanced Science Engineering Information Technology*, **7**, 3, 964
2. ATAEI M., ASADI E., GOODARZI A., KHAJEPOUR A., KHAMESEE M.B., 2017, Multi-objective optimization of a hybrid electromagnetic suspension system for ride comfort, road holding and regenerated power, *Journal of Vibration and Control*, **23**, 5, 782-793
3. BALZARINI D., ZAABAR I., CHATTI K., 2017, Impact of concrete pavement structural response on rolling resistance and vehicle fuel economy, *Transportation Research Record Journal of the Transportation Research Board*, **2640**, 84-94
4. BENTO A.M., GILLINGHAM K., ROTH K., 2017, The effect of fuel economy standards on vehicle weight dispersion and accident fatalities, *NBER Working Papers*, **23340**
5. BROWNE A., HAMBURG J., 1986, On road measurement of the energy dissipated in automotive shock absorbers, *Symposium on Simulation and Control of Ground Vehicles and Transportation Systems*, Anaheim CA, USA, **80**, 2, 167-186
6. CHEN D.-H., JIN X.-X., 2004, Analytical study on nonlinear model for tire stiffness and damping, *Chinese Journal of Construction Machinery*, **2**, 4, 408-412
7. DAVID S.B., BOBROVSKY B.Z., 2011, Actively controlled vehicle suspension with energy regeneration capabilities, *Vehicle System Dynamics*, **49**, 6, 833-854
8. DONG D., HUANG W., BU F., WANG Q., 2017, Analysis and optimization of a tubular permanent magnet linear motor using transverse-flux flux-reversal topology, *International Conference on Electrical Machines and Systems*, 1-5
9. HSU C.T., HUANG G.Y., CHU H.S., YU B., YAO D.-J., 2011, Experiments and simulations on low-temperature waste heat harvesting system by thermoelectric power generators, *Applied Energy*, **88**, 4, 1291-1297

10. HUANG S., XU X., 2017, A regenerative concept for thermoelectric power generation, *Applied Energy*, **185**, 119-125
11. JI X.W., GAO Y.M., QIU X.D., 1994, The dynamic stiffness and damping characteristics of the tire, *Automotive Engineering*, **16**, 5, 315-321
12. KO J., KO S., SON H., YOO B., CHEON J., KIM H., 2015, Development of brake system and regenerative braking cooperative control algorithm for automatic-transmission-based hybrid electric vehicles, *IEEE Transactions on Vehicular Technology*, **64**, 2, 431-440
13. LI L., ZHANG Y., YANG C., YAN B., MARTINEZ C.M., 2016, Model predictive control-based efficient energy recovery control strategy for regenerative braking system of hybrid electric bus, *Energy Conversion and Management*, **111**, 299-314
14. LI Z., ZUO L., KUANG J., LUHRS G., 2013, Energy-harvesting shock absorber with a mechanical motion rectifier, *Smart Material Structures*, **22**, 2, 025008
15. LV C., ZHANG J., LI Y., YUAN Y., 2015, Mechanism analysis and evaluation methodology of regenerative braking contribution to energy efficiency improvement of electrified vehicles, *Energy Conversion and Management*, **92**, 469-482
16. MO J.S., QIU Z.C., WEI J.Y., ZHANG X.M., 2017, Adaptive positioning control of an ultrasonic linear motor system, *Robotics and Computer-Integrated Manufacturing*, **44**, 156-173
17. NAKANO K., SUDA Y., NAKADAI S., 2003, Self-powered active vibration control using a single electric actuator, *Journal of Sound and Vibration*, **260**, 2, 213-235
18. SHI D., PISU P., CHEN L., WANG S., WANG R., 2016, Control design and fuel economy investigation of power split HEV with energy regeneration of suspension, *Applied Energy*, **182**, 576-589
19. SINGAL K., RAJAMANI R., 2013, Zero-energy active suspension system for automobiles with adaptive sky-hook damping, *Journal of Vibration and Acoustics*, **135**, 1, 011011
20. YU S., DU Q., DIAO H., SHU G., JIAO K., 2015, Start-up modes of thermoelectric generator based on vehicle exhaust waste heat recovery, *Applied Energy*, **138**, 276-290
21. ZUO L., SCULLY B., SHESTANI J., ZHOU Y., 2010, Design and characterization of an electromagnetic energy harvester for vehicle suspensions, *Smart Material Structures*, **19**, 4, 1007-1016